Proceedings of the 21^{th} National & 10^{th} ISHMT-ASME Heat and Mass Transfer Conference

December 27 - 30, 2011,IIT, Madras,India

ISHMT-IND-04-003

Effect of buoyancy on oscillatory flow in a vertical pipe

Ashwin T.R
Dept. of Mechanical Engineering
Indian Institute of Science, Bangalore
Bangalore, India- 560 012
Email: ashwin@mecheng.iisc.ernet.in

G. S. V. L. Narasimham*
Dept. of Mechanical Engineering
Indian Institute of Science, Bangalore
Bangalore, India- 560 012
Email: mecgsvln@mecheng.iisc.ernet.in

Subhash Jacob
Centre for Cryogenic Technology
Indian Institute of Science, Bangalore
Bangalore, India- 560 012
Email: jacob@ccf.iisc.ernet.in

(* Corresponding Author)

Abstract

The effect of natural convection on the oscillatory flow in an open-ended pipe driven by a time-wise sinusoidally varying pressure at one end and subjected to an ambient-to-cryogenic temperature difference across the ends, is numerically studied. Conjugate effects arising out of the interaction of oscillatory flow with heat conduction in the pipe wall are taken into account by considering a finite thickness wall with an insulated exterior surface. Two cases, namely, one with natural convection acting downwards and the other, with natural convection acting upwards, are considered. Parametric studies are conducted with frequencies in the range 5-15 Hz for an end-to-end temperature difference of 200 K and 50 K.

Keywords: Pulse tube, Natural convection, Conjugate conduction.

Introduction

Oscillating flow problems have practical applications in equipment like Stirling engines and refrigerators, regenerators, combustor pipes, pulse tube coolers, pipe manifolds and in biological systems in relation to blood flow. The effect of natural convection on the oscillating flow is important in devices like pulse tubes with a cold heat exchanger of cryogenic temperature at one end and ambient hot heat exchanger at the other end. The work reported in the area of natural convection in pipes is mostly confined to through flow produced by buoyancy in vertical and inclined pipes. A few studies have considered pipes with closed ends. The present authors have earlier considered the problem of oscillating flow and heat transfer in an open tube with negligible buoyancy forces (Ashwin et al., 2011). Hence the results reported are applicable to a horizontal pipe or for situations with negligible gravity. However, for vertical geometries, the effect of buoyancy becomes important, which is the subject of the present study. The study is performed with low pressure amplitudes with buoyancy acting upward and downward to differentiate the effect of natural convection in oscillating flows.

Natural convection in a vertical cylinder with adiabatic lateral walls with constant but different temperatures on the end surfaces has been studied numerically by He et al. (2004). Other contributions relevant to oscillating flows are Faghri et al. (1979), Guo et al., (1997) and Chattopadhyay et al., (2006). These are already covered in Ashwin et al. (2011).

Formulation

Geometry

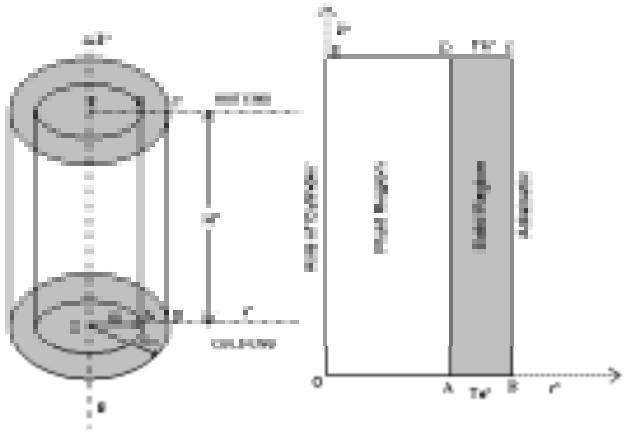

Figure 1: Physical model and coordinate system

Fig. 1 shows the physical model and coordinate system. Cylindrical polar coordinate system is chosen with the assumption of axisymmetric flow and temperature distributions. The model consists of a cylindrical pipe open at both ends, with a finite wall thickness. Two configurations are studied. In the first one the gravity vector is parallel to the z-axis and acts vertically downwards (i.e. the angle between gravity vector and z-axis is 180°). The other one is an inverted configuration with the gravity vector acting vertically upwards (i.e. the angle between the gravity vector and z-axis is 0°). The working medium at the ends of the tube is assumed to be isothermal but at different temperatures. For example, these regions correspond to the cold and warm heat exchangers of a pulse tube refrigerator. The working medium when entering one of the ends does so at a cryogenic temperature T_e, while the working medium entering the other end of the tube is at a higher temperature T_h (typically room temperature). The oscillating flow in the tube is driven by a sinusoidally varying pressure at the cold end of the tube. Since the so called DC component is absent, the fluid flow during a cycle takes place partly into and partly out of the tube at either end. The height of the tube and the inner and outer radii are H, R_i and R_o, respectively. Clearly the wall thickness δ_w is $R_\mathrm{o} - R_\mathrm{i}$. The oscillating heat transfer between the wall and the gas is taken into account through the coupling between the fluid and the solid at the interface. The annular surfaces of the solid at the tube ends are assumed to be insulated.

Non-dimensionalisation

The characteristic length L_c is taken as the inner radius R_i of the tube and the characteristic temperature T_c as the hot heat exchanger temperature T_h, which is also the ambient temperature. The geometrical parameters of the problem are the dimensionless inner radius R_i^* of the tube, dimensionless height H^* and the dimensionless wall thickness δ_w^*. The characteristic density ρ_c corresponds to the state of helium at the charge pressure p_o and ambient temperature $T_\mathrm{h} = T_\mathrm{c}$. The characteristic thermal conductivity, specific heat and dynamic viscosity of the working medium, i.e. helium gas, correspond to T_c and are denoted respectively k_c, $c_\mathrm{p,c}$ and μ_c. The dimensionless temperature T^* is $(T - T_\mathrm{c})/\Delta T_\mathrm{c}$ where ΔT_c is $T_\mathrm{h} - T_\mathrm{e}$. The quantity $\epsilon = \Delta T_\mathrm{c}/T_\mathrm{c}$ is the overheat ratio. The characteristic pressure is p_c is taken as $\rho_\mathrm{c} v_\mathrm{c}^2$ where v_c, the characteristic velocity, is taken as ωL_c, the quantity ω being the angular frequency. The time is non-dimensionalised with the time period of the oscillation $1/\omega$. Thus the dimensionless time period t_p^* is 2π.

The dimensionless quantities are defined as:

$$
\begin{aligned}
&t^* = t\omega,\ r^* = \frac{r}{L_\mathrm{c}},\ z^* = \frac{z}{L_\mathrm{c}},\ L_\mathrm{c} = R_\mathrm{i} \\
&v_\mathrm{r}^* = \frac{v_\mathrm{r}}{v_\mathrm{c}},\ v_\mathrm{z}^* = \frac{v_\mathrm{z}}{v_\mathrm{c}},\ p^* = \frac{p}{\rho_\mathrm{c} v_\mathrm{c}^2},\ v_\mathrm{c} = \omega L_\mathrm{c} \\
&T^* = \frac{T - T_\mathrm{c}}{\Delta T_\mathrm{c}},\ \epsilon = \frac{\Delta T_\mathrm{c}}{T_\mathrm{c}},\ \Delta T_\mathrm{c} = T_\mathrm{h} - T_\mathrm{e} \\
&\rho^* = \frac{\rho}{\rho_\mathrm{c}},\ c_\mathrm{p}^* = \frac{c_\mathrm{p}}{c_\mathrm{p,c}},\ \mu^* = \frac{\mu}{\mu_\mathrm{c}},\ k^* = \frac{k}{k_\mathrm{c}} \\
&Re = \frac{v_\mathrm{c} L_\mathrm{c} \rho_\mathrm{c}}{\mu_\mathrm{c}},\ Pr = \frac{\mu_\mathrm{c} c_\mathrm{p,c}}{k_\mathrm{c}},\ Ec = \frac{v_\mathrm{c}^2}{c_\mathrm{p,c} T_\mathrm{c}} \\
&Gr_c = \frac{g\epsilon L_c^3}{\nu_c^2}\ H^* = \frac{H}{L_\mathrm{c}},\ \delta_\mathrm{w}^* = \frac{\delta_\mathrm{w}}{L_\mathrm{c}}
\end{aligned}
$$

The dimensionless outer radius is $R_\mathrm{o}^* = R_\mathrm{o}/L_\mathrm{c} = (R_\mathrm{i} + \delta_\mathrm{w})/L_\mathrm{c} = R_\mathrm{i}^* + \delta_\mathrm{w}^* = 1 + \delta_\mathrm{w}^*$ (since $R_\mathrm{i}^* = 1$) and the dimensionless charge pressure $p_\mathrm{o}^* = p_\mathrm{o}/(\rho_\mathrm{c} v_\mathrm{c}^2)$. The dimensionless properties should correspond to the fluid or solid depending upon the region under consideration, i.e. the working medium or wall. Thus the dimensionless ratios, namely, μ_f^*, $c_\mathrm{p,f}^*$ and k_f^*, the subscript 'f' denoting fluid, are assigned a value of unity in the fluid domain. In the solid region, the property values should correspond to those of the solid, namely, k_s^* and $c_\mathrm{s}^* = c_\mathrm{s}/c_\mathrm{p,c}$. In the numerical analysis, the solid is treated as a fluid of infinite viscosity.

Dimensionless governing equations

The dimensionless continuity, momentum and energy equations are as follows:

Continuity equation

$$\frac{\partial \rho^*}{\partial t^*} + \frac{1}{r^*}\frac{\partial}{\partial r^*}(r^*\rho^* v_{\mathrm{r}}^*) + \frac{\partial}{\partial z^*}(\rho^* v_{\mathrm{z}}^*) = 0$$

Momentum equation in the radial direction

$$\frac{\partial}{\partial t^*}(\rho^* v_{\mathrm{r}}^*) + \frac{1}{r^*}\frac{\partial}{\partial r^*}(r^*\rho^* v_{\mathrm{r}}^* v_{\mathrm{r}}^*) + \frac{\partial}{\partial z}(\rho^* v_{\mathrm{z}}^* v_{\mathrm{r}}^*) = -\frac{\partial p^*}{\partial r^*} + \frac{1}{Re}\left[\frac{1}{r^*}\frac{\partial}{\partial r^*}\left(r^*\mu^*\frac{\partial v_{\mathrm{r}}^*}{\partial r^*}\right) + \frac{\partial}{\partial z^*}\left(\mu_*\frac{\partial v_{\mathrm{r}}^*}{\partial z^*}\right)\right] + \frac{1}{Re}\left[\frac{\partial}{\partial z^*}\left(\mu^*\frac{\partial v_{\mathrm{z}}^*}{\partial r^*}\right) + \frac{1}{r^*}\frac{\partial}{\partial r^*}\left(r^*\mu^*\frac{\partial v_{\mathrm{r}}^*}{\partial r^*}\right) - \frac{2\mu^* v_{\mathrm{r}}^*}{r^{*2}} - \frac{2}{3}\frac{\partial}{\partial r^*}(\mu^* D^*)\right] + \frac{Gr_c}{{Re_{R,c}}^2}\frac{1}{\epsilon}((\rho^*-1)\vec{g}.\vec{e_r})$$

Momentum equation in axial direction

$$\frac{\partial}{\partial t^*}(\rho^* v_{\mathrm{z}}^*) + \frac{1}{r^*}\frac{\partial}{\partial r^*}(r^*\rho^* v_{\mathrm{r}}^* v_{\mathrm{z}}^*) + \frac{\partial}{\partial z^*}(r^*\rho^* v_{\mathrm{z}}^* v_{\mathrm{z}}^*) = -\frac{\partial p^*}{\partial z^*} + \frac{1}{Re}\left[\frac{1}{r^*}\frac{\partial}{\partial r^*}\left(r^*\mu^*\frac{\partial v_{\mathrm{z}}^*}{\partial r^*}\right) + \frac{\partial}{\partial z^*}\left(\mu^*\frac{\partial v_{\mathrm{z}}^*}{\partial z^*}\right)\right] + \frac{1}{Re}\left[\frac{\partial}{\partial z^*}\left(\mu_*\frac{\partial v_{\mathrm{z}}^*}{\partial z^*}\right) + \frac{1}{r^*}\frac{\partial}{\partial r^*}\left(r^*\mu^*\frac{\partial v_{\mathrm{r}}^*}{\partial z^*}\right) - \frac{2}{3}\frac{\partial}{\partial r^*}(\mu^* D^*)\right] + \frac{Gr_c}{{Re_c}^2}\frac{1}{\epsilon}((\rho^*-1)\vec{g}.\vec{e_z})$$

Energy equation

$$\frac{\partial}{\partial t^*}(\rho^* T^*) + \frac{1}{r^*}\frac{\partial}{\partial r^*}(\rho^* r^* v_{\mathrm{r}}^* T^*) + \frac{\partial}{\partial z^*}(\rho^* v_z^* T^*) = \frac{1}{RePr}\left[\frac{1}{r^*}\frac{\partial}{\partial r^*}\left(\frac{k^*}{c_{\mathrm{p}}^*}r^*\frac{\partial T^*}{\partial r^*}\right) + \frac{\partial}{\partial z^*}\left(\frac{k^*}{c_{\mathrm{p}}^*}\frac{\partial T^*}{\partial z^*}\right)\right] + \frac{Ec}{c_{\mathrm{p}}^*\,\epsilon}\frac{Dp^*}{Dt^*}$$

Equation of state

$$p^* = \frac{1}{Ec}\,\rho^*\,\frac{\gamma-1}{\gamma}(T^*\,\epsilon + 1)$$

The dimensionless divergence is given by:

$$D^* = \frac{1}{r^*}\frac{\partial}{\partial r^*}(r^* v_{\mathrm{r}}^*) + \frac{\partial v_{\mathrm{z}}^*}{\partial z^*}$$

The substantive derivative Dp^*/Dt^* is given by:

$$\frac{Dp^*}{Dt^*} = \frac{\partial p^*}{\partial t^*} + v_{\mathrm{r}}^*\frac{\partial p^*}{\partial r^*} + v_{\mathrm{z}}^*\frac{\partial p^*}{\partial z^*}$$

The pressure oscillation at the inlet of the pipe is:

$$p^*(t^*) = p_{\mathrm{o}}^* + p_{\mathrm{a}}^*\sin(t^*)$$

where p_o^* is the dimensionless charge pressure.

Initial and boundary conditions

It is assumed that at the beginning (i.e. $t^* = 0$), the geometry is under ambient condition and the system is filled with helium gas at the charge pressure. These conditions are taken as 300 K and 25 bar.

No-slip and zero mass permeability is assumed on the solid boundary in contact with the fluid. Oscillating pressure and zero radial velocity are prescribed at the cold end of the tube. At the hot end of the tube, zero streamwise derivative of the radial velocity is prescribed. The axial velocities at the inlet and outlet are calculated using the continuity equation. On the axis of the tube, zero cross-stream derivative of the axial velocity and zero radial velocity are imposed.

At the interface between the solid and the fluid, heat flux continuity and no temperature jump conditions should be satisfied. This is done through the harmonic mean thermal conductivity method. At the cold end, the temperature condition is taken as the cold heat exchanger temperature when the flow takes place into the tube and as zero axial temperature gradient when the flow is out of the tube. Similar conditions are also applied at the hot end of the tube. Since the pipe is oriented in a vertical direction, there is no contribution of buoyancy in the r-direction because $\vec{g}.\vec{e_r} = 0$.

Parametric Studies

The numerical method, grid dependency study and validation of the computer code are reported in an earlier paper (Ashwin et al., 2011). The numerical experimentation is conducted for a tube with length of 100 mm and diameter 8 mm. Thus the length-to-diameter ratio of the tube is kept constant. Two end temperature differences, 200 K and 50 K, are tested, keeping the hot end at a constant value of 300 K and choosing the cold end temperature as 250 K and 100 K. The corresponding Rayleigh number based on diameter of the pipe ranges form 4.87×10^6 for 200 K temperature and 1.22×10^6 for 50 K temperature difference. The frequency ranges from 5 to 15 Hz.

Results and Discussion

The effect of orientation on temperature profiles

Figs. 2(a) and 2(b) show the temperature contours inside the tube after attaining steady periodic

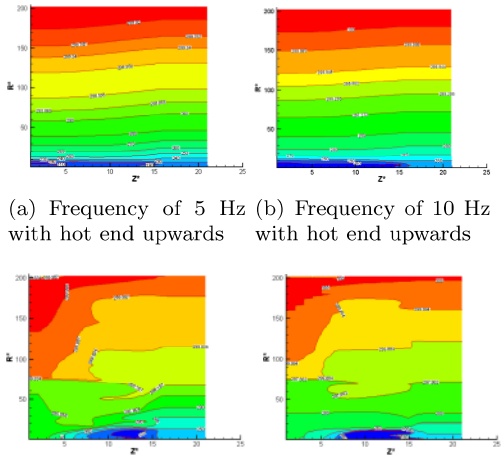

(a) Frequency of 5 Hz with hot end upwards

(b) Frequency of 10 Hz with hot end upwards

(c) Frequency 5 Hz hot end downwards

(d) Frequency 10 Hz hot end downwards

Figure 2: Temperature profiles for $Ra = 4.87 \times 10^6$

condition with hot end at the top for the higher Rayleigh number. The pressure amplitude is 50 Pa. The isotherms in the profiles are smooth and vertical to the wall and the axis in the major part of the tube. They are very crowded near the cold end where sharp temperature gradients exist. The hot end and the middle cross section of the tube show more uniform temperature compared to the region near the cold end. The outer wall of the tube is kept at adiabatic condition. But there is always heat transfer between solid and the wall inside the tube. Figs. 2(c) and 2(d) show the temperature profiles with hot end at the bottom. It can be seen that the smoothness in the isotherms is completely lost and there is considerable distortion in the profiles due to the influence of natural convection occurring in the tube due to the placement of hot end at the lower side. Thus this configuration tends to destroy the temperature gradient in the tube, making the temperature in the middle portion more or less uniform. There is an upward flow of gas due to the positioning of hot end downwards. Near the wall, the isotherms are still smooth and vertical. The results show that the positioning of hot and cold heat exchangers is important in pulse tube refrigerators. The general conclusion is that for any type of open tubes with similar configuration, three main zones can be identified. The cold gas zone near the cold end, a hot gas zone near the hot end and a central buffer zone separating the above mentioned zones. Placing the hot heat exchanger at the bottom will smear the temperature gradient in the tube and will result in mixing of gases inside the tube which will decease the efficiency.

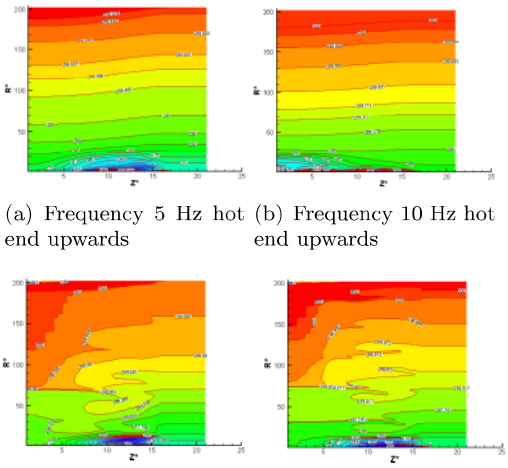

(a) Frequency 5 Hz hot end upwards

(b) Frequency 10 Hz hot end upwards

(c) Frequency 5 Hz hot end downwards

(d) Frequency 10 Hz hot end downwards

Figure 3: Temperature profiles for $Ra = 1.22 \times 10^6$

Fig. 3 shows similar set of results for the lower Rayleigh number. The profiles are almost similar to Fig. 2. The profiles at frequencies of 5 Hz and 10 Hz also look almost similar for both the Rayleigh numbers.

Fig. 4 shows the variation of cross-sectionally averaged axial velocity and temperature for 5 Hz frequency for 50 Pa pressure amplitude after attaining steady periodic condition for $Ra = 4.9 \times 10^6$ at the middle cross-section of the tube. The temperature profiles in Fig. 4(a) show a temperature oscillation between 296.5 K and 296.2 K when the hot end is at the top. With cold end at the top, the temperature oscillates between 299.9 K and 299.69 K. Clearly this behavior in the temperature oscillation is due to the influence of natural convection. Cold end temperature is found to be diffusing more into the middle section for first configuration and hot end temperature is more diffusing for the second configuration. This is due to the fact that the configuration with hot end down will aid the natural convection effect and keeps the middle cross section nearer to hot end temperature. It is conjectured that at higher pressure amplitudes, the periodic flow effect suppresses the natural convection effect. The velocity profiles are shown in Fig. 4(b) for both the configurations. For hot side up configuration, the velocities are oscillating in positive and negative directions. Thus for hot end at top configuration, the velocity is experiencing oscillation.

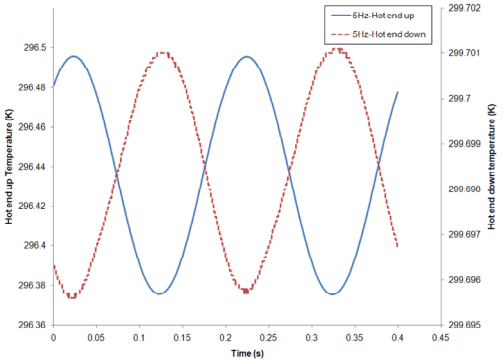

(a) Temperature Variation

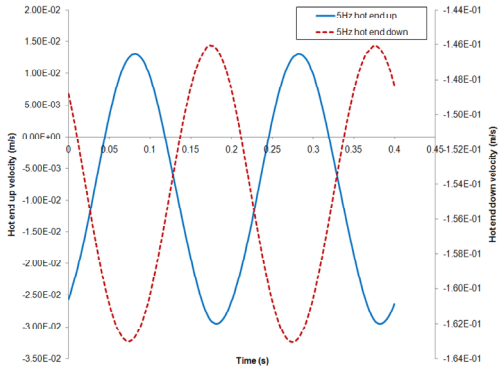

(b) Velocity variation

Figure 4: Temperature and velocity variations for 5 Hz frequency 50 Pa amplitude during steady periodic conditions.

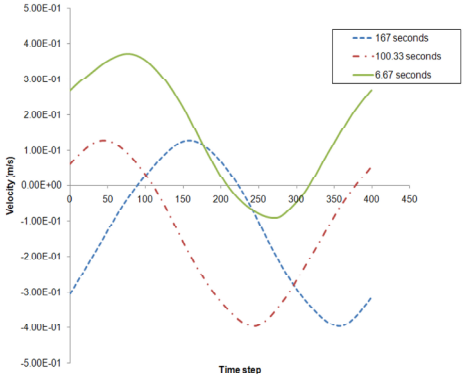

(a) Hot end up

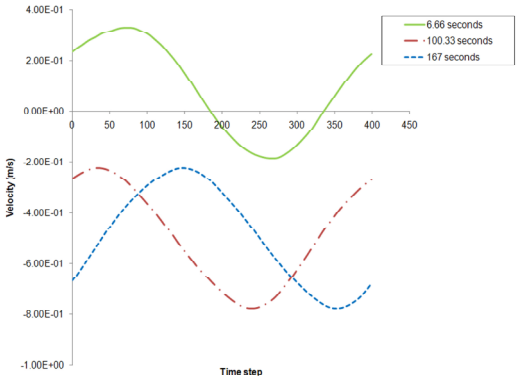

(b) Hot end down

Figure 5: Velocity plot for 15 Hz frequency and P_a=500 Pa.

But for hot end bottom configuration, the buoyancy overpowers the oscillatory flow producing a unidirectional flow.

Velocity and Nusselt number variations

Fig. 5 shows the area-averaged velocity variation inside the tube for 500 Pa pressure amplitude at 15 Hz for $Ra = 1.22 \times 10^6$ at the cold end. Fig. 6 shows the correponding Nusselt number variation. The results correspond to times of 6.66, 100.33 and 167 seconds after the startup. From Figs. 5(a) and 5(b), the profiles have positive and negative parts in a cycle in the beginning, for instance, after 6.66 seconds. This means that the gas inside the tube tube oscillates (i.e. moves in both directions) and experiences a complete flow reversal in the beginning. The profiles after 100.33 seconds and 167 seconds show some deviation from the first profile. This is more clear in the second figure 5(b). The major change is that the positive portion decreases and negative contribution increases. This can be due to the change in density due to cooldown and also the effect of natural convection acting on the tube. There is a diffusion of cold end temperature into the tube and the density inside the tube changes rapidly. Velocity profiles in the cases with hot end down (Fig. 5(b)) have only negative flow contributions after attaining steady periodic condition and still the oscillating nature persists.

The behavior in velocity profiles can be explained as follows. Assuming that there is a constant part and variable part for the velocity oscillation, the variable part is due to the sinusoidal driving force at the inlet of the tube and the constant part is due to the effect of natural convection. Since this is an open tube, natural convection will occur either upwards or downwards depending on the temperature difference. The variable part of velocity will experience changes due to the variation in density. The

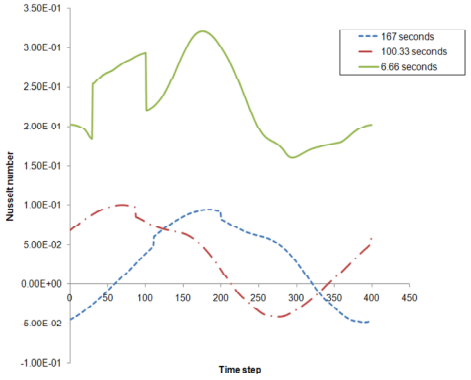

(a) Hot end up

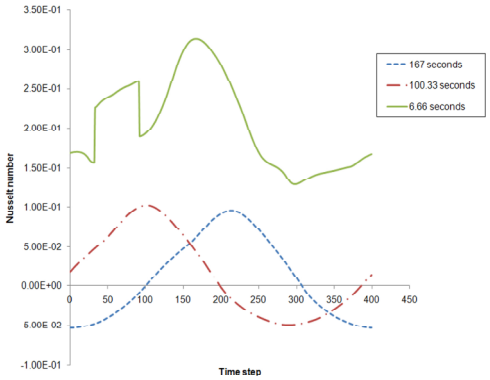

(b) Hot end down

Figure 6: Nusselt number plot for 15 Hz frequency and P_a=500 Pa.

constant part or unidirectional part, due to the influence of natural convection, is mainly controlled by change in density changes inside the tube (or Rayleigh number), orientation and boundary conditions. The balance of the two effects determines the oscillating nature of gas inside the tube. In the the first case (Fig. 5(a)) the velocity variation is controlled mainly by the pressure oscillation at inlet and in the second case (Fig. 5(b)), by the effect of natural convection. The negative dominance of velocity in Fig. 5(b) is due to the pushing of gas downwards due to the very low cold end temperature (and hence higher density) compared to the hot end.

Fig. 6 shows the variation of Nusselt number over one cycle with hot end facing up as well as down. It can be seen that the average Nusselt number variation is not affected much by the orientation and that it becomes smoother as more time elapses from the startup. The value of Nusselt number increases and decreases during a cycle, positive Nusselt number indicating heat transfer from wall to gas. The variation in the Nusselt number follows the same pattern as that of the average velocity over one cycle. Although there is gas-to-solid surface heat pumping in the tube, this quantity will be small compared to pressure heat pumping (i.e. enthalpy flow). However, surface heat pumping can become significant in high frequency pulse tube refrigerators.

Conclusions

Numerical methods are found to be capable of predicting the contours of temperature, velocity, etc, inside the oscillating flow tube for the cases under consideration. The distortion in isothermal lines are found to be more when hot end is placed down. It is therefore advisable to keep the hot end up for better functioning of devices like pulse tube coolers wherein this kind of conditions are encountered. The variation of Nusselt number and velocity is smooth for zero Rayleigh number cases, but sharp changes in these quantities are observed when natural convection comes into play.

References

[1] Ashwin, T.R., Narasimham, G.S.V.L., Jacob, S., 2011. Oscillatory flow and temperature fields in an open tube with temperature difference across the ends, International Journal of Heat and Mass Transfer 54 3357-3368.

[2] He, Y.L., Tao, W.Q., Qu, Z.G., Chen,Z.Q., 2004. Steady natural convection in a vertical cylindrical envelope with adiabatic lateral wall, International Journal of Heat and Mass Transfer 47 3131-3144.

[3] Faghri, M., Javdani, K., Faghri, A., 1979. Heat transfer with laminar pulsating flow in a pipe, Letters in Heat and Mass Transfer 6 259-270.

[4] Guo, Z., Sung, H.J., 1997. Analysis of the Nusselt number in pulsating pipe flow, International Journal of Heat and Mass Transfer 40 2486-2489.

[5] Chattopadhyay, H., Durst, F., Ray, S., 2006. Analysis of heat transfer in simultaneously developing pulsating laminar flow in a pipe with constant wall temperature, International Communications in Heat and Mass Transfer 33 475-481.